Journal of Theoretical Biology 494 (2020) 110214

Contents lists available at ScienceDirect

Journal of Theoretical Biology

journal homepage: www.elsevier.com/locate/jtb

Quantifying nutrient throughput and DOM production by algae in continuous culture

A.W. Omta[a,*], D. Talmy[b], K. Inomura[c], A.J. Irwin[d], Z.V. Finkel[e], D. Sher[f], J.D. Liefer[g], M.J. Follows[a]

[a] Department of Earth, Atmospheric and Planetary Sciences, Massachusetts Institute of Technology, 77 Massachusetts Avenue, Cambridge, MA 02139, United States
[b] Department of Microbiology, University of Tennessee, 1311 Cumberland Avenue, Knoxville, TN 37916, United States
[c] School of Oceanography, University of Washington, 1492 NE Boat Street, Seattle, WA 98105, United States
[d] Department of Mathematics and Statistics, Dalhousie University, 6316 Coburg Road, Halifax, NS B3H 4R2, Canada
[e] Department of Oceanography, Dalhousie University, 1355 Oxford Street, Halifax, NS B3H 4R2, Canada
[f] Department of Marine Biology, Leon H. Charney School of Marine Sciences, University of Haifa, 199 Aba Khoushy Avenue, Mount Carmel 3498838, Haifa, Israel
[g] Department of Biology, Mount Allison University, 63B York Street, Sackville, NB E4L 1G7, Canada

ARTICLE INFO

Article history:
Received 21 March 2019
Revised 7 November 2019
Accepted 24 February 2020
Available online 4 March 2020

Keywords:
Algal stoichiometry
Plankton physiology
DOM production
Plankton model

ABSTRACT

Freshwater and marine algae can balance nutrient demand and availability by regulating uptake, accumulation and exudation. To obtain insight into these processes under nitrogen (N) and phosphorus (P) limitation, we reanalyze published data from continuous cultures of the chlorophyte *Selenastrum minutum*. Based on mass budgets, we argue that much of the non-limiting N and P had passed through the organisms and was present as dissolved organic phosphorus or nitrogen (DOP or DON). We construct a model that describes the production of biomass and dissolved organic matter (DOM) as a function of the growth rate. A fit of this model against the chemostat data suggests a high turnover of the non-limiting N and P: at the highest growth rates, N and P atoms spent on average only about 3 h inside an organism, before they were exuded as DON and DOP, respectively. This DOM exudation can explain the observed trends in the algal stoichiometric ratios as a function of the dilution rate. We discuss independent evidence from isotope experiments for this apparently wasteful behavior and we suggest experiments to quantify and characterize DON and DOP exudation further.

1. Introduction

The elemental stoichiometry (C:N:P ratio) of the algae at the base of aquatic food webs is of fundamental importance for their functioning, as it impacts the growth rates of zooplankton (Plath and Boersma, 2001; Boyer et al., 2004; Hessen et al., 2013) and bacteria (Del Giorgio and Cole, 1998; Lønborg et al., 2011). Although the average C:N:P ratio of organic matter in the ocean is relatively constant (Redfield, 1934), the elemental stoichiometry of algae and organic particles varies significantly in space and time (Donald et al., 2001; Körtzinger et al., 2001; Martiny et al., 2013; Singh et al., 2015). To capture such variations, we need to understand how the elemental stoichiometry of algae is related to their growth rate and environment.

Algal stoichiometry ultimately reflects the flow of nutrients through the organisms. It has been known for a long time that regulation of nutrient uptake and internal allocation of nutrients are important in this regard (Rhee, 1973; 1974) and these processes have been central in various algal physiological models (Shuter, 1979; Geider et al., 1998; Pahlow, 2005; Smith and Yamanaka, 2007; Pahlow and Oschlies, 2009). In addition, exudation of dissolved organic matter (DOM) is known to be important and has been included in several phytoplankton models. In some of these models, exudation is simply a fixed fraction of the uptake or biomass (Fasham et al., 1990; Vallino, 2000; Anderson and Pondaven, 2003; Pahlow et al., 2008; Grossowicz et al., 2017a),

* Corresponding author.
E-mail addresses: omta@mit.edu (A.W. Omta), dtalmy@utk.edu (D. Talmy), ki24@uw.edu (K. Inomura), a.irwin@dal.ca (A.J. Irwin), zfinkel@dal.ca (Z.V. Finkel), dsher@univ.haifa.ac.il (D. Sher), jliefer@mta.ca (J.D. Liefer), mick@ocean.mit.edu (M.J. Follows).

https://doi.org/10.1016/j.jtbi.2020.110214

whereas it is related to the internal reserves or nutrient quota in others (Lorena et al., 2010; Ghyoot et al., 2017; Grossowicz et al., 2017b; Livanou et al., 2019). Flynn et al. (2008) fitted models based on both types of formulations to batch culture data on several algal species (Biddanda and Benner, 1997; Clark, 1998), finding that either formulation could describe the data well. Furthermore, Flynn et al. (2008) estimated that 0–30% of the gross C and N uptake is released as DOM, thus underlining the importance of exudation from a mass-budget perspective.

What could be the combined impact of nutrient uptake regulation, internal allocation, and exudation on algal stoichiometry? To gain insight into this question, we consider the canonical Elrifi and Turpin (1985) chemostat experiments, in which the C:N:P ratios of the green alga *Selenastrum minutum* were measured under severe N and P limitation for a large range of dilution rates. The Elrifi and Turpin (1985) experiments provided one of the most comprehensive studies of cellular N and P responses to steady-state nutrient limitation, but have proven difficult to model and interpret. According to the Growth Rate Hypothesis (GRH), the P content of algae and other organisms should increase with increasing growth rate, because maintaining high growth rates requires a high complement of P-rich ribosomes (Elser et al., 1996; Sterner and Elser, 2002; Vrede et al., 2004; Moody et al., 2017). However, the N:P ratio under N limitation decreases with increasing growth rate: exactly the opposite of would be expected from the GRH (Flynn et al., 2010). Such breakdowns of the GRH can occur, if ribosomal RNA accounts for only a small fraction of the total P quota of phytoplankton (Moreno and Martiny, 2018). Under N limitation and P oversupply, much P may accumulate into intracellular pools other than RNA or DNA, such as polyphosphates. Thus, the dynamics of *non-limiting* nutrients likely need to be represented in a model to reproduce and understand the Elrifi and Turpin (1985) measurements. This is in contrast with the classical Droop (1968) model commonly used to interpret algal stoichiometric data, which considers the relationship between the *limiting* nutrient quota and the growth rate of the organisms (Flynn, 2008).

Here, we revisit the Elrifi and Turpin (1985) dataset with a combination of mass budgets and chemostat modeling, interpreting a fast, growth-rate dependent flux of non-limiting N or P and then discuss the implications. Using the mass budgets (Section 2), we argue that a significant fraction of the non-limiting N and P may have been in DON and DOP in these experiments. Therefore, our model formulation (Section 3) includes exudation of N and P, as well as uptake regulation and allocation of N and P to protein and RNA. Previously, the Elrifi and Turpin (1985) data have been fit with models using two different approaches (Flynn, 2008; Bougaran et al., 2010). The Flynn (2008) model used auxiliary variables, such as the P:C ratio at which P transport is repressed (PC_{rep}). For a good fit to the N-limited chemostat measurements, this variable needed to have a parabolic dependence on the N:C ratio of the organisms. That is, as the N:C ratio became higher, PC_{rep} first increased and then decreased, without a clear biochemical underpinning. Bougaran et al. (2010) did not include such auxiliary variables and focused on uptake regulation mechanisms. In this model, N uptake was regulated by both the N and the P quota, because N uptake requires ATP and cofactors containing P. By contrast, P uptake was regulated by the P quota alone and not by the N quota, which seems consistent with observations (Karl, 2014; Lin et al., 2016). However, the Bougaran et al. (2010) model did not achieve as good a fit as the Flynn (2008) model, in particular under N limitation. Thus, it appears that the inclusion of uptake regulation mechanisms is not sufficient to model the N:P trends observed by Elrifi and Turpin (1985). In our model, we represent not only uptake regulation but also exudation, a process that is known to occur, which neither Flynn (2008) nor Bougaran et al. (2010) included. This allows us to fit the data using fewer parameters than either Flynn (2008) or Bougaran et al. (2010). In Section 4, we use our model to estimate uptake and exudation rates of N and P for the Elrifi and Turpin (1985) experiments. These estimated rates are high and increase with increasing growth rate. The parameter estimate suggests that at the highest growth rates, N and P atoms spend on average only a few hours inside the organisms before they are exuded. Finally, we discuss various lines of empirical evidence pertaining to exudation and turnover of N and P among phytoplankton and we discuss possible reasons for a high exudation (Section 5).

2. Mass budgets

In this section, we first provide a brief summary of the Elrifi and Turpin (1985) measurements, after which we perform mass-budget calculations based on these measurements. We use the inferences from these mass budgets to inform the structure of our model describing the cycling of N and P between the medium and the organisms (Section 3).

Elrifi and Turpin (1985) performed chemostat measurements on the chlorophyte *Selenastrum minutum* under N and P limitation. In such experiments, input medium containing known concentrations of nutrients is added at a certain rate, while the culture containing organisms and residual nutrients is diluted out at the same rate. Since the culture is at steady state, the growth rate of the organisms equals the dilution rate. In other words, both the nutrient supply (and therefore the severity of nutrient limitation) and the growth rate of the organisms are controlled by the dilution rate. One problem in various chemostat experiments has been that the algal cells tend to take up all the non-limiting N or P as luxury consumption (e.g., Rhee, 1978; Healey, 1985; Terry et al., 1985). Elrifi and Turpin (1985) avoided this by using input medium with extremely high and extremely low N:P ratios: 2 mM KNO_3 and 10 μM Na_2HPO_4, i.e., an N:P ratio of 200:1 (P limitation) and 100 μM KNO_3 and 100 μM Na_2HPO_4, i.e., an N:P ratio of 1:1 (N limitation). The algae were unable to deplete the non-limiting nutrient, because it was simply too overabundant. Elrifi and Turpin (1985) measured particulate C, N, and P, total chlorophyll, and residual nitrate and phosphate in the outflow medium.

The mass budgets are illustrated in Fig. 1. At all dilution rates, Elrifi and Turpin (1985) found residual non-limiting nutrient concentrations in the range of 40–60 μM for phosphate or 1.25–1.50 mM for nitrate. These measurements were well above the detection limit of the relevant assays (Elrifi and Turpin, personal communication). In the N-limited experiments, the N:P ratio of the particulate organic matter was ~2 at low dilution rates, increasing to ~10 at the highest dilution rates. Assuming that all the 100 μM N in the input medium was converted into biomass, this means that P in biomass amounted to ~50 μM at low dilution rates and ~10 μM at the highest dilution rates. Since the total amount of P equaled 100 μM, the residual phosphate (40–60 μM) and biomass P (~50 μM) can together account for all the P at low dilution rates. However, there emerges a gap in the mass budget at high dilution rates: the residual phosphate (40–60 μM) and biomass P (~10 μM) add up to only 50–70 μM, which implies that 30–50 μM P is unaccounted for. Similarly, there is a gap in the N budget at high dilution rates under P limitation. Assuming that all the limiting P was in biomass, the amount of non-limiting N in biomass was ~0.15 mM at the highest dilution rates, because the N:P ratio of the particulate organic matter was around 15 and the P in the input medium was 0.01 mM. This means that the biomass N and nitrate add up to 1.40–1.65 mM. Since the input medium contained 2.0 mM N, 0.35–0.60 mM N is not accounted for.

How could the gaps in the budgets of non-limiting N and P be explained? It is common for especially P in particular to disap-

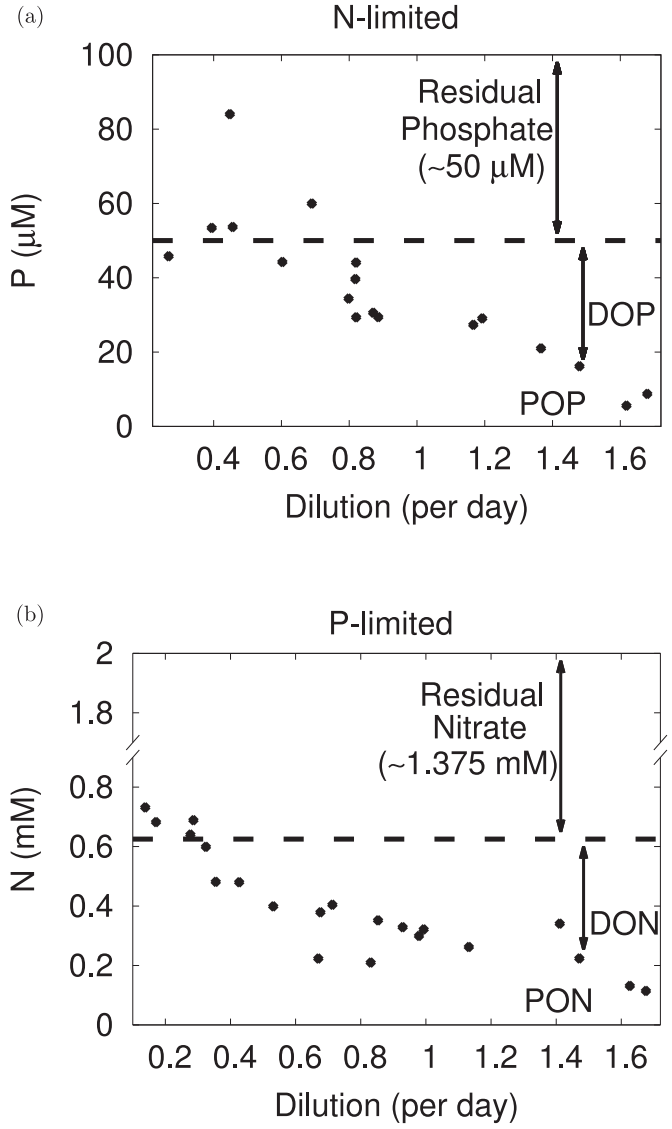

Fig. 1. The P budget under N limitation (a) and the N budget under P limitation (b). The P (a) and N (b) above the dashed line are accounted for by the residual phosphate (a) and nitrate (b); the P (a) and N (b) underneath the data points are accounted for by POM, under the assumption that all the limiting N (a) and limiting P (b) are in POM. The gap between the data points and the dashed line at the higher dilution rates may then be accounted for by DOM.

pear from microalgae growth media when precipitates form during preparation. However, this depends (among other things) on the major cations used in the experiments, which were Na^+ and K^+ (Elrifi and Turpin, 1985). Na_2HPO_4 and K_2HPO_4 are highly soluble in water, up to 0.5 M and 3.5 M, respectively (Eysseltova and Dirkse, 1988): about 4 orders of magnitude higher than the concentrations used. Moreover, P precipitation during preparation would have led to a gap in the P budget at all growth rates. As can be seen in Fig. 1a, there is only a significant gap in the P budget at growth rates over 1 per day and there is no budget gap at low growth rates. Budget gaps could also be caused by measurement errors, but it is again unclear why such budget gaps would systematically increase with increasing growth rate of the organisms. This suggests that the cause of the budget gaps was in the culture. In other words, some of the non-limiting P/N that was added would have been converted in the culture into forms that were neither inorganic P/N nor particulate P/N. Such forms can be defined operationally as DOM (Koistinen et al., 2020), even if they are not necessarily organic molecules (e.g., polyphosphate is DOP according to this operational definition).

Assuming that the missing N and P was in DOM, further inferences can be made. Firstly, the DOM exudation must have increased with increasing growth rate, because the DOM concentration increased with increasing growth rate. A DOM exudation rate independent of the growth rate would have led to a DOM concentration that decreased with increasing growth/dilution rate, as the DOM was lost from the chemostat faster at higher dilution. Secondly, the uptake rates of the non-limiting nutrients must have been higher at high dilution rates than at low dilution rates. Without such a variation in the uptake rates, the concentration of residual non-limiting nitrate and phosphate would have increased with increasing dilution rate, because the supply rate of nutrients is also higher at higher dilution rates. Probably, this variation in the uptake of the non-limiting nutrients is due to downregulation at the low dilution rates because of the very high internal quota of these nutrients.

3. Model

Early models for algal physiology and stoichiometry focused on the role of the internal quota of a single nutrient (Droop, 1968; Caperon and Meyer, 1972), an approach that was later expanded to multiple nutrients (Legovic and Cruzado, 1997; Klausmeier et al., 2004). More recently, there has been emphasis on nutrient uptake regulation (Pahlow, 2005; Smith and Yamanaka, 2007) and the internal allocation of nutrients to various functional macromolecular pools (Smith and Yamanaka, 2007; Pahlow and Oschlies, 2009). The Flynn (2008) and Bougaran et al. (2010) models, which were used to interpret the Elrifi and Turpin (1985) experiments, also had a strong focus on the regulation of nutrient uptake and transport. Relatively little attention has been paid to exudation, although models may provide a more accurate description of cellular growth if this process is explicitly included (Kooijman, 2010; Grossowicz et al., 2017a). In fact, the mass budgets in the previous section indicate that in the Elrifi and Turpin (1985) experiments, a large fraction of the non-limiting N and P taken up by the organisms was exuded as DON and DOP. Therefore, both uptake regulation and exudation are represented in our chemostat model. Furthermore, the model includes the generally observed increase in the RNA:protein ratio with increasing growth rate (Scott et al., 2010).

Our model (schematic in Fig. 2, with parameters and variables in Tables 1 and 2, respectively) includes N and P in the medium (N_{med} and P_{med}), C, N and P in living biomass (C_{bio}, N_{bio}, and P_{bio}), divided into pools of functional RNA and protein (N_{RNA} and N_{prot}, in N units), and C, N, and P reserves (C_{res}, N_{res}, and P_{res}). The reason for this division is that the rates of nutrient uptake and biomass production are determined by the functional pools, while the reserve pools likely play a key role in determining the overall C:N:P ratios of the organisms. Furthermore, we assume that the nutrient uptake rate is proportional to the amount of protein. With inflow N and P concentrations N_{in} and P_{in} and chemostat dilution rate d, we have the following dynamic equations for N_{med} and P_{med}:

$$\frac{dN_{med}}{dt} = d(N_{in} - N_{med}) - V_N N_{prot} \tag{1}$$

$$\frac{dP_{med}}{dt} = d(P_{in} - P_{med}) - V_P N_{prot} \tag{2}$$

The uptake rates of both N and P follow Michaelis-Menten kinetics; uptake regulation is included through a linearized version

Table 1
Description of the parameters with associated units and first-guess and posterior values; wherever the posteriors have no error estimates, the parameter has been held constant. The uncertainty measure is one standard deviation.

Symbol	Description	Initial guess	Posterior	Units
$P_{m,C}$	Maximum gross photosynthesis rate	20	33.2 ± 1.3	mol C/N-mol protein per day
$V_{m,N}$	Maximum N uptake rate	10	8.6 ± 0.4	mol N/N-mol protein per day
$V_{m,P}$	Maximum P uptake rate	5	1.31±0.04	mol P/N-mol protein per day
$K_{C,i}$	Photosynthesis inhibition saturation constant	2	15.6 ± 0.2	mol C/mol N
$K_{N,i}$	N uptake inhibition saturation constant	2	1.437±0.014	–
$K_{P,i}$	P uptake inhibition saturation constant	2	0.540±0.010	mol P/mol N
$y_{Ex,N,0}$	N excretion fraction at $\mu = 0$	0.1	0.0002±0.0012	–
a_N	Increase in N excretion fraction with increasing μ	0.1	0.467±0.007	days
$y_{Ex,P,0}$	P excretion fraction at $\mu = 0$	0.1	0.00001±0.00016	–
a_P	Increase in P excretion fraction with increasing μ	0.1	0.515±0.003	days
b_0	RNA:protein at $\mu = 0$	0.06	0.06	N-mol RNA/N-mol protein
b_1	Increase in RNA:protein with increasing μ	0.08	0.08	N-mol RNA/N-mol protein days
r_0	Maintenance respiration	0.1	0.1	per day
r_1	Respiration cost of growth	0.3	0.3	–
$R_{C:N(DON)}$	C:N ratio of DON	2	3.1 ± 0.4	mol C/mol N
$R_{C:P(DOP)}$	C:P ratio of DOP	2	6.6 ± 0.9	mol C/mol P
$R_{N:P(RNA)}$	N:P ratio of RNA	3.75	3.75	mol N/mol P

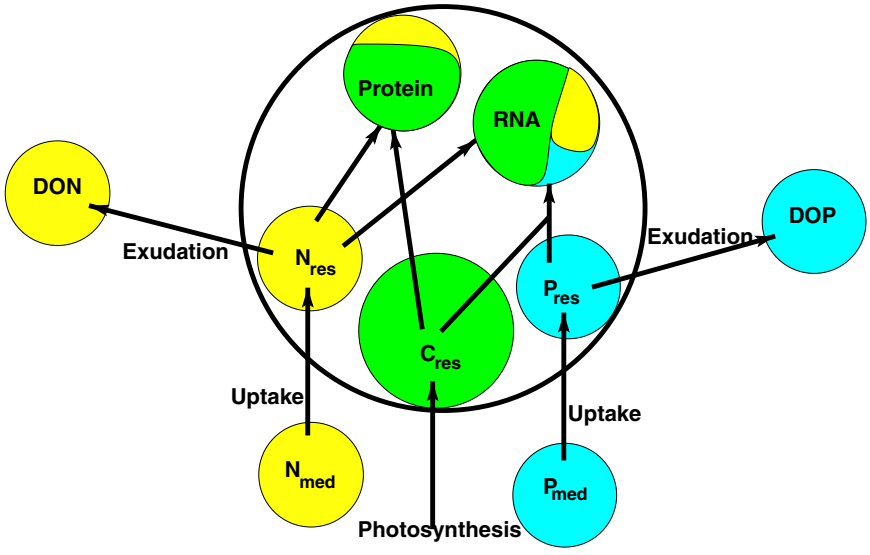

Fig. 2. A schematic depiction of the model with the different compartments: DIN and DIP in the medium (N_{med} and P_{med}), protein (N_{prot}), RNA (N_{RNA}/P_{RNA}), N and P reserves (N_{res} and P_{res}), DON, DOP. N_{prot}, N_{RNA}, and N_{res} together form N_{bio}; P_{RNA} and P_{res} together form P_{bio}. The colors indicate the different elements: green for C, yellow for N, blue for P. (For interpretation of the references to color in this figure legend, the reader is referred to the web version of this article.)

of the Rhee (1973) uptake regulation formulation:

$$V_N = \frac{V_{m,N}N_{med}}{K_N + N_{med}} \frac{1}{1 + \frac{Q_{N,i}}{K_{N,i}}} \approx \frac{V_{m,N}N_{med}}{K_N + N_{med}} \left(1 - \frac{Q_{N,i}}{K_{N,i}}\right) \quad (3)$$

$$V_P = \frac{V_{m,P}P_{med}}{K_P + P_{med}} \frac{1}{1 + \frac{Q_{P,i}}{K_{P,i}}} \approx \frac{V_{m,P}P_{med}}{K_P + P_{med}} \left(1 - \frac{Q_{P,i}}{K_{P,i}}\right) \quad (4)$$

with K_N and K_P half-saturation constants for the uptake of N and P, respectively, and $V_{m,N}$ and $V_{m,P}$ respective maximum uptake rates for N and P. $Q_{N,i}$ and $Q_{P,i}$ are the total N and P inside the organisms, normalized by the amount of N in functional biomass: $Q_{N,i} \equiv N_{bio}/(N_{prot}+N_{RNA})$, $Q_{P,i} \equiv P_{bio}/(N_{prot}+N_{RNA})$, whereas $K_{N,i}$ and $K_{P,i}$ are coefficients determining the uptake inhibition (Rhee, 1973). Our linearized Eqs. (3) and (4) are analogous to the formulation for P uptake regulation used by Bougaran et al. (2010). In contrast with Bougaran et al. (2010), the formulation for uptake regulation is qualitatively the same for N and P. We are making this choice, because using the same formulation for N and P is the simplest and most parsimonious approach. Moreover, the residual non-limiting inorganic nutrient concentration is approximately constant across all dilution rates under both N and P limitation in the Elrifi and Turpin (1985) experiments, suggesting that uptake regulation operates in a similar fashion for both nutrients.

The N and P taken up are assimilated into biomass with yield factors y_N and y_P:

$$\frac{dN_{bio}}{dt} = y_N V_N N_{prot} - dN_{bio} \quad (5)$$

$$\frac{dP_{bio}}{dt} = y_P V_P N_{prot} - dP_{bio} \quad (6)$$

The remaining fractions $y_{Ex,N} \equiv 1\text{-}y_N$ and $y_{Ex,P} \equiv 1\text{-}y_P$ are released as DON and DOP, essentially the same formulation as in the

Table 2
Description of the variables with associated units.

Symbol	Description	Units
N_{med}	N in medium	mM N
P_{med}	P in medium	µM P
C_{res}	C in storage	µM C
N_{res}	N in storage	µM N
P_{res}	P in storage	µM P
C_{RNA}	C in RNA	µM C
N_{RNA}	N in RNA	µM N
P_{RNA}	P in RNA	µM P
C_{prot}	C in protein	µM C
N_{prot}	N in protein	µM N
C_{bio}	C in biomass	µM C
N_{bio}	N in biomass	µM N
P_{bio}	P in biomass	µM P
d	Dilution rate	per day

classical Fasham et al. (1990) model. Furthermore, mass budgets (Fig. 1) suggest that the exuded fractions increase with increasing growth rate (μ). As a first-order approximation, we assume that this increase is linear:

$$y_{Ex,N} = y_{Ex,N,0} + a_N \mu \tag{7}$$

$$y_{Ex,P} = y_{Ex,P,0} + a_P \mu \tag{8}$$

with $a_N \equiv d(y_{Ex,N})/d\mu$, $a_P \equiv d(y_{Ex,P})/d\mu$ constants.

The dynamics of biomass C (C_{bio}) are determined by the balance of gross photosynthesis (P_C), respiration (r_C), C exudation (ex_C), the costs of DON production due to the required NO_3^- reduction (co_{DON}), and dilution:

$$\frac{dC_{bio}}{dt} = P_C - r_C - ex_C - co_{DON} - dC_{bio} \tag{9}$$

We assume that photosynthesis is proportional to the amount of protein and is regulated by the C quota of the organisms in a manner analogous to how the uptake of N and P is regulated by the N and P quota:

$$P_C = \frac{P_{m,C} N_{prot}}{1 + \frac{Q_{C,i}}{K_{C,i}}} \approx P_{m,C} N_{prot} \left(1 - \frac{Q_{C,i}}{K_{C,i}}\right) \tag{10}$$

with $Q_{C,i} \equiv C_{bio}/(N_{prot}+N_{RNA})$. We do not account for variations in the light intensity, since the light intensity was constant in the Elrifi and Turpin (1985) experiments. We use an empirical formula for respiration, taking account of both maintenance and growth respiration:

$$r_C = (r_0 + r_1 \mu) C_{bio} \tag{11}$$

Geider and Osborne (1989) compiled values for the maintenance respiration and growth respiration parameters for various algal species. Here, we will use average values from this compilation, taking r_0 equal to 0.1 per day and r_1 equal to 0.3.

We take $ex_C = R_{C:N(DON)}(1\text{-}y_N)V_N N_{prot} + R_{C:P(DOP)}(1\text{-}y_P)V_P N_{prot}$, with $R_{C:N(DON)}$ the C:N ratio of the exudate under P limitation and $R_{C:P(DOP)}$ the C:P ratio of the exudate under N limitation. Furthermore, we take $co_{DON} = 2(1\text{-}y_N)V_N N_{prot}$: we assume that producing 1 mol of dissolved organic N from nitrate costs (the equivalent of) 2 mol C. The reason for this assumption is that the energetic costs of the conversion of nitrate into biomass N are ~12 mol ATP/(mol N) (Raven, 1984; Pahlow, 2005), while aerobic glucose oxidation produces ~6 mol ATP/(mol C) (Rich, 2003). Together, this gives an estimate for the respiratory costs of protein synthesis of ~2 mol C/mol N.

To calculate the division between the different macromolecular pools within the biomass, we assume that the limiting nutrient is entirely in the functional components (protein+RNA for N, RNA for P). The RNA:protein ratio increases with the growth rate (consistent with the GRH), according to an empirical relationship:

$$\frac{N_{RNA}}{N_{prot}} = b_0 + b_1 \mu \tag{12}$$

We take b_0 equal to 0.06 N-mol RNA/N-mol protein and b_1 equal to 0.08 N-mol RNA/N-mol protein days, based on observations on the protist *Euglena gracilis* (Cook, 1963); similar relationships exist for various other microorganisms (Figure S1 in Scott et al., 2010). We take the N:P ratio of RNA ($R_{N:P(RNA)}$) equal to 3.75, because the nucleobases of RNA have on average 3.75 N atoms: adenine and guanine each have 5, cytosine has 3, and uracil has 2 N atoms.

As described in detail in Appendix A, these equations give rise to expressions for the stoichiometric ratios under N and P limitation and the residual non-limiting nitrate and phosphate in the medium, which are then fitted against the chemostat data. The parameter estimation is performed using a Metropolis et al. (1953) procedure, as described in Appendix B and discussed in Omta et al. (2017). For our parameter estimation, we use not only the reported algal stoichiometric ratios (C:N, C:P, N:P), but also their inverses (N:C, P:C, P:N) to prevent the data points with high C or N from dominating the fit. Based on a visual inspection of the data, we assume uncertainties for the N-limited measurements of 0.4 mol C/mol N, 0.003 mol N/mol C, 3 mol C/mol P, 0.0015 mol P/mol C, 0.5 mol N/mol P, 0.05 mol P/mol N, and 5 µM respectively for the C:N, N:C, C:P, P:C, N:P, P:N ratios, and residual phosphate, and for the P-limited measurements 0.4 mol C/mol N, 0.01 mol N/mol C, 25 mol C/mol P, 0.001 mol P/mol C, 4 mol N/mol P, 0.003 mol P/mol N, and 62.5 µM respectively for the C:N, N:C, C:P, P:C, N:P, P:N ratios, and residual nitrate.

4. Results

The fits are shown in Fig. 3. The purple model curves are composed of 500 randomly drawn simulations with parameter sets accepted by the Metropolis algorithm. As a result, the widths of the composite purple curves reflect the uncertainties in the fits. Twelve parameters are estimated: the maximum photosynthesis rate $P_{m,C}$, the maximum N and P uptake rates $V_{m,N}$ and $V_{m,P}$, the inhibition coefficients $K_{C,i}$, $K_{N,i}$, and $K_{P,i}$, the exudation parameters $y_{Ex,N,0}$, a_N, $y_{Ex,P,0}$, and a_P, the C:N ratio of DON $R_{C:N(DON)}$, and the C:P ratio of DOP $R_{C:P(DOP)}$. The means and standard deviations of the posterior parameter distributions are listed in Table 1; as an example, one posterior parameter distribution (of $V_{m,P}$) is plotted in Fig. 4. The estimated maximum N and P uptake rates (8.6 ± 0.4 mol N/N-mol protein per day and 1.31±0.04 mol P/N-mol protein per day, respectively) are lower than the maximum uptake rates for *Selenastrum minutum* measured in pulse experiments: ~12 mol N/N-mol protein per day for N (Weger et al., 1988) and ~3 mol P/N-mol protein per day for P (Gauthier and Turpin, 1997). Possibly, the organisms in the pulse experiments were hoarding N and P temporarily, whereas the populations in the Elrifi and Turpin (1985) continuous culture experiments were at steady state. For the other estimated parameters (e.g., DOM production), no such direct comparison can be made with measured values, but we will discuss evidence pertaining to DOM production on a more general level in Section 5.

Our chemostat model captures key trends observed by Elrifi and Turpin (1985). Consistent with the data, the C:N ratio decreases and the C:P and N:P ratios increase with increasing dilution under N limitation (Fig. 3a, c, e), the C:N, C:P, and N:P ratios all decrease with increasing dilution under P limitation (Fig. 3b, d, f), and the concentration of the non-limiting residual phosphate is approximately constant (Fig. 3g). The non-limiting residual nitrate increases slightly and reaches a plateau (Fig. 3h), but remains mostly

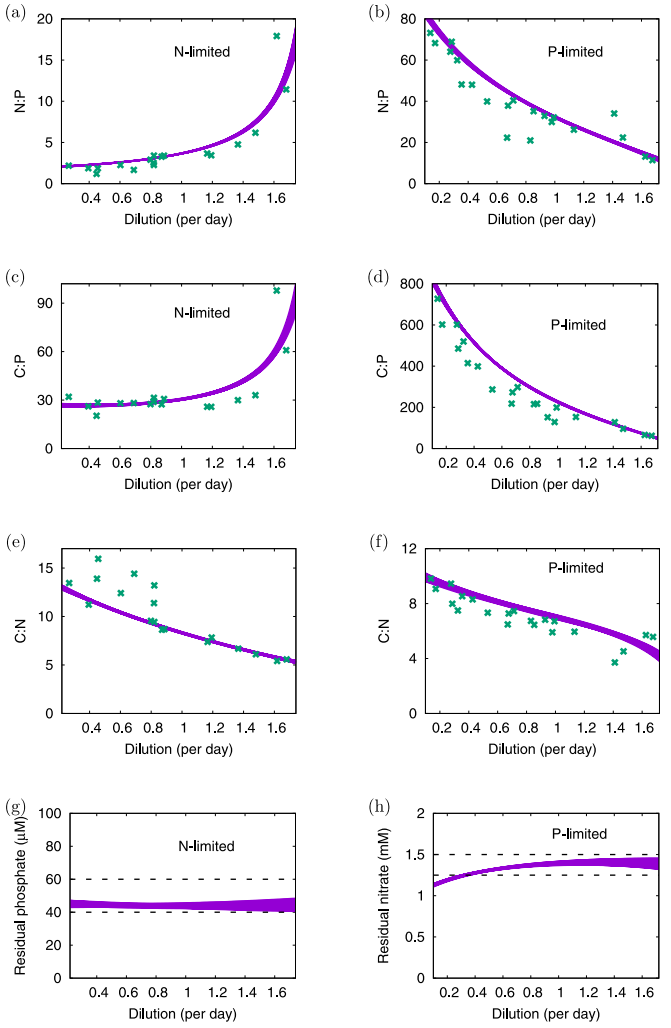

Fig. 3. (a,b,c,d,e,f) Model fits (purple lines) and chemostat measurements (green crosses) on *Selenastrum minutum* (Elrifi and Turpin, 1985): N:P under N (a) and P limitation (b); C:P under N (c) and P limitation (d); C:N under N (e) and P limitation (f). (g,h) Model fits (purple lines) and measured boundaries (dashed black lines) of phosphate under N limitation (g) and nitrate under P limitation (h). Each of the purple model curves is composed of 250 randomly drawn simulations with parameter sets accepted by the Metropolis algorithm. The widths of the composite lines reflect the uncertainties in the fits, according to the algorithm. (For interpretation of the references to color in this figure legend, the reader is referred to the web version of this article.)

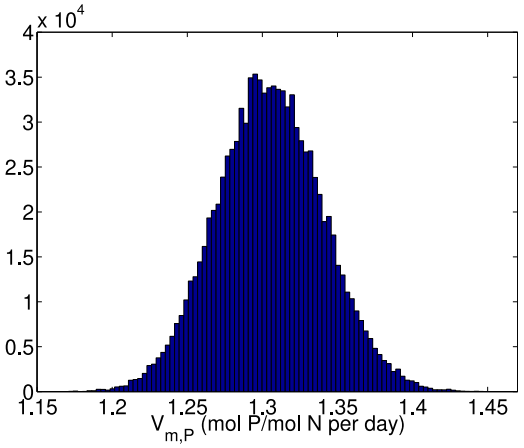

Fig. 4. An example of a posterior parameter distribution ($V_{m,P}$).

within the 1.25–1.5 mM measured by Elrifi and Turpin (1985). The parameter estimate indicates that the fraction of the non-limiting N and P taken up that is exuded as DON and DOP increases from about 10% at the lowest growth rates up to 80% at the highest growth rates. Essentially, such a high exudation is needed to be consistent with the mass budgets. At the highest growth rates, more non-limiting N and P is in DOM than in living biomass (see Fig. 1), implying that most of the non-limiting nutrients taken up must be converted into DOM. Furthermore, we have estimated elemental turnover rates by dividing the amount of C, N, and P in biomass by the exudation rates of each of these elements. These estimates indicate that at the highest growth rates, non-limiting N and P atoms spent on average about 3 h inside an organism before being exuded. By comparison, the turnover of C estimated by our model is relatively slow: at the highest growth rates, C atoms spent on average about 1 day (N limitation) or about 6 h (P limitation) inside an organism before being exuded.

5. Discussion

Algae can manage the flow of nutrients such as N and P in various ways. To examine the potential roles of nutrient uptake regulation, internal allocation, and exudation, we have reanalyzed the Elrifi and Turpin (1985) measurements on the chlorophyte *Selenastrum minutum* in continuous culture. We inferred that there were gaps in the mass budgets of the non-limiting N and P. Mass budget gaps could be caused by precipitation during preparation of the growth medium or by measurement errors, but such gaps would likely have been independent of the algal growth rate. The fact that the mass budget gaps systematically increase with increasing algal growth rate suggests to us that the cause of the budget gaps must be sought in the algal culture. A possible explanation is then that the algae converted a large fraction of the non-limiting N and P into DON and DOP, in particular at the highest growth rates. A formal parameter estimate using a plankton model then suggested that DOM exudation played a key role in determining the N:P ratios. That is, the exudation was lowest at low growth rates, leading to a large accumulation of non-limiting N and P. At higher growth rates, exudation was higher, leading to lower N:P ratios under P limitation and higher N:P ratios under N limitation. In the following, we will first discuss issues related to the interpretation of our mass budgets (Section 5.1). Subsequently, we will address existing empirical evidence pertaining to exudation and turnover of N and P, as well as possible future experiments to test our inferences (Section 5.2). Finally, we will focus on why organisms may exude DOM at high rates (Section 5.3).

5.1. Interpretation of the mass budgets

Our mass budgets rely on a comparison between the inorganic N and P in the input medium on one hand and the particulate N and P and the residual inorganic N and P on the other hand. This may not be entirely accurate for P, since the inorganic P concentration in the completed media can be overestimated when using standard measurement procedures (Benitez-Nelson, 2000). Thus, the P budget gap may have been larger than we estimated. In that case, both the DOP concentration and the DOP production rate would have been even higher than we inferred.

Which N- and P-rich molecules would the organisms have accumulated at low dilution rates and exuded at higher dilution rates in the Elrifi and Turpin (1985) experiments? One indication is provided by the N-limited N:P ratios at low dilution rates. These ratios were so low (around 2) that much P must have been in molecules that do not contain N, such as polyphosphates. Indeed, it has been observed that a large portion of phytoplankton cellular P is allocated to polyphosphates (Rhee 1973; Powell et al., 2011), even in

oceanic environments where P is very scarce (Orchard et al., 2010; Martin et al., 2014; Diaz et al., 2016). Moreover, the green alga *Chlamydomonas reinhardtii* has been observed to release polyphosphates into its extracellular matrix (Werner et al., 2007). NMR measurements on the DOP produced by the diatom *Thalassiosira pseudonana* (Saad et al., 2016) have suggested that most of the DOP consisted of phosphate esters. Apart from phosphate esters, exudation of phosphonates and phosphites (Van Mooy et al., 2015) and nucleic acids (Biller et al., 2014) has been found, depending on the phytoplankton species. The molecular composition of DON exuded by phytoplankton seems less variable, with much being in the form of amino acids (Hammer and Brockmann, 1983; Admiraal et al., 1986; Myklestad et al., 1989), although exudation in the form of ammonium (Bergman, 1984) and nucleic acids (Biller et al., 2014) has also been observed. That said, it is questionable whether the molecular composition of the DOM released in the Elrifi & Turpin (1985) experiments would have been similar to what has been observed in these other studies. That is, the Elrifi and Turpin, 1985 experiments were performed under rather extreme input medium N:P ratios equal to 1:1 (N limitation) and 200:1 (P limitation). Thus, the organisms received a large excess of N (P limitation) and P (N limitation) with nowhere to put it, which may have led to exudation of DOM with low C:N (P limitation) and C:P (N limitation). Indeed, our parameter estimates indicate low DOM C:N and C:P ratios of 3.1 $\pm$ 0.4 and 6.6 $\pm$ 0.9, respectively (see Table 1). As a corollary, the inferred high rates of DON and DOP production might occur only when there is a large overabundance of N or P. Such overabundance is uncommon in the natural environment, although inorganic N:P ratios varying between values as low as 0.2 and as high as 260 have been recorded in eutrophic lakes (Barica, 1990). Even so, fast turnover of P has been observed in various natural ecosystems. P turnover times in lakes vary between 1 min and 1 week, depending on the trophic state and the season (Rigler, 1964; Halmann and Stiller, 1974; Peters and MacIntyre, 1976; Boulion, 2012). Turnover times in the open ocean are on the order of 1–10 days (Benitez-Nelson and Buesseler, 1999; Björkman et al., 2000; Nausch and Nausch, 2006; Nowlin et al., 2007; Paytan and McLaughlin, 2007; Sohm and Capone, 2010; Björkman et al., 2012), significantly longer than the few hours that we estimated. However, the open-ocean measurements may in many cases reflect the turnover through the entire microbial loop, rather than the residence time within one organism.

5.2. Empirical evidence

Is there independent evidence that algae excrete large amounts of DON and DOP? A survey of various culture studies indicated that phytoplankton release on average ~20% of their gross N uptake as DON (Sipler and Bronk, 2015), with the exact fraction depending on various factors such as the nutritional state of the organisms (Bronk, 1999; Nagao and Miyazaki, 2002). It appears that phytoplankton exudes DON mainly in the form of amino acids (Sipler and Bronk, 2015). Experiments using radiolabeled P suggest high rates of rapid P uptake and excretion for various organisms. Maximum P uptake rates more than 100-fold greater than what would be required stoichiometrically for growth were found for the chlorophyte *Dunaliella salina* (Grant et al., 2013) and for the diatom *Thalassiosira weissflogii* (Laws et al., 2013). Exudation measurements have indicated a fast P release on a timescale of minutes, followed by a slower release on timescales of hours to days for both the ciliate *Strombidium viride* (Taylor and Lean, 1981) and the green alga *Scenedesmus quadricauda* (Jansson, 1993). Dissolved organic phosphorus (DOP) production coupled with P uptake has been documented in a variety of natural ecosystems. For example, Björkman et al. (2000) observed that 10–40% of the net P uptake in the subtropical North Pacific is released as dissolved organic phosphorus (DOP). Björkman and Karl (2003) then estimated that the microbial community in the North Pacific subtropical gyre derives ~50% of its P from DOP. In mesocosm experiments, P enrichment led to a high DOP production, with most of the added inorganic P having been converted into DOP within 3–5 days (Ruttenberg and Dyhrman, 2012). Even so, the actual mechanisms behind DOP production and the specific contribution from excretion by phytoplankton remain elusive (Karl and Björkman, 2015). Further evidence regarding exudation rates may be collected through batch culture studies, in which the accumulation of N- and P-rich compounds is monitored. Apart from being an empirical test for our inferred rapid N and P exudation, such measurements could provide insight into the key physiological processes. A different starting point for more detailed investigations may be pulse-and-chase isotope measurements. However, exudation rates may be underestimated in such experiments due to re-uptake of exuded DOM, since many phytoplankton species produce DON and DOP hydrolysis enzymes, e.g., amine oxidases (Palenik and Morel, 1991; Pantoja and Lee, 1994) and alkaline phosphatase (Litchman and Nguyen, 2008; Ranhofer et al., 2009; Dyhrman, 2016; Li et al., 2016).

Our parameter estimate suggests that there was significant exudation of C, in addition to N and P exudation. Furthermore, the production of large amounts of DON under P limitation would have implied the reduction of large amounts of NO_3^-. Was the light intensity in the experiments (100 μE/(m^2 s)) sufficient to sustain the estimated rates of organic matter production? To investigate this, we calculated the required gross photosynthesis rates (see Appendix C). This required gross photosynthesis turned out to be highest at high growth rates under P limitation, reaching about 0.5 mol C/(g Chl hr). Similar, and even higher, C fixation rates have been observed in cultures under 100 μE/(m^2 s) (e.g., Platt et al., 1980; Harding et al., 1982; Felcmanová et al., 2017), as well as in the natural environment (Laws et al., 2016). Note that the gross photosynthesis is actually higher than these measured C fixation rates, which do not include respiration. In addition, the maximum photosynthesis rates predicted by the model are within the expected range based on the turnover number of Rubisco (see detailed calculation in Appendix C). Thus, empirical evidence suggests that the gross photosynthesis required to sustain the organic matter production rates is not implausible.

5.3. Why would organisms exude N and P at high rates?

From an ecological perspective, there may be benefits to exudation due to mutualisms and competition. For example, Berman-Frank and Dubinsky (1999) suggested that phytoplankton could benefit from exuding DOC because of mutualistic relationships with bacteria. It has been suggested that the cyanobacterium *Trichodesmium* exudes P-rich compounds for this reason (Van Mooy et al., 2015). Furthermore, the bacterium *Azospirillum brasilense* has been shown to enhance polyphosphate exudation by the green alga *Chlorella vulgaris* (Meza et al., 2015). In many cases, the costs of producing and exuding compounds that benefit a mutualist appear negligible (Pacheco et al., 2019). Alternatively, organisms may rapidly take up non-limiting P to deprive competitors of this resource; the purpose of the DOP release is then simply to get rid of the excess P. This could be a viable strategy, because much of the DOP released by phytoplankton is refractory: for example, phosphonates, organophosphates, and organophosphites are not degraded by phosphatases. It is more difficult to see how such a strategy could work in the case of N, since phytoplankton exude N mostly in labile forms (amino acids, ammonium, nucleic acids).

Taking a more physiological perspective, the origin of the inferred increase in DOM production with increasing growth rate may be that a faster metabolism produces more waste. However,

it could also indicate a shift to different metabolic pathways. For example, bacteria and yeast have been observed to shift from an oxidative metabolism at low growth rates to a fermentative ("overflow") metabolism at high growth rates, even in the presence of sufficient oxygen (Rieger et al., 1983; Sonnleitner and Kappeli, 1986; Majewski and Domach, 1990; Szenk et al., 2017). This shift then leads to an increase in exudation of acetate and ethanol, as well as a decreasing biomass yield per amount of substrate. It has been argued that this shift occurs, because the costs of synthesizing the required enzymes become more important than the metabolic efficiency of the pathway at high substrate concentrations (Molenaar et al., 2009). Indeed, the costs of synthesizing the required proteins have been shown to be higher for respiration than for fermentation (Basan et al., 2015). Could similar metabolic shifts be responsible for the increase in DON and DOP exudation with increasing growth rate inferred from the Elrifi and Turpin (1985) measurements? The generality and specifics of this question, brought forth by the analysis presented here, could be addressed through dedicated experiments and modeling efforts. Particularly helpful may be chemostat experiments on phytoplankton, in which the molecular composition of the exuded DON and DOP is analyzed at different growth rates. Subsequently, the possible metabolic origins of changes in the exuded molecules may be investigated using Flux Balance Analysis (Orth et al., 2010).

Data archiving

This study did not generate any new data, as it used published chemostat measurements (Elrifi and Turpin, 1985). The FORTRAN code and the data that were used are available through https://github.com/AWO-code/ElrifiTurpin1985.

Acknowledgments

The authors would like to thank Dave Turpin, Ivor Elrifi, Harold Weger, and two anonymous reviewers for helpful comments and discussions. This work was supported by the Simons Collaboration on Computational Biogeochemical Modeling of Marine Ecosystems/CBIOMES (Grant ID: 549931, MJF). Furthermore, the authors are grateful for support from the Gordon & Betty Moore Foundation [Grant number GBMF #3778], the National Science Foundation [Grant numbers NSF-OCE-1315201, NSF-OCE-1536521 to DT and MJF], the Simons Foundation [Simons Postdoctoral Fellowship in Marine Microbial Ecology, Award 544338, KI], the Natural Sciences and Engineering Research Council of Canada to AJI and ZVF, and the United States-Israel Binational Science Foundation [Grant number 2010183 to DS and MJF].

Appendix A. Chemostat at steady state

We solve the steady-state equations directly by setting the time derivatives equal to 0, as is commonly done in Metabolic Flux Models (Varma and Palsson, 1994) and we set the growth rate μ equal to the dilution rate d. Below, we make approximations based on which nutrient is limiting.

A.1. P limitation

We assume that all the P is in RNA: $P_{RNA} = P_{bio} = P_{in}$. Eq. (12) then gives:

$$N_{prot} = \frac{N_{RNA}}{b_0 + b_1 d} = \frac{R_{N:P(RNA)} P_{in}}{b_0 + b_1 d} \tag{A.1}$$

with $R_{N:P(RNA)}$ the N:P ratio of RNA. N_{med} is very high (1.25–1.5 mM) under P limitation, which means that Eq. (3) for the N uptake can be approximated as:

$$V_N \approx V_{m,N}\left(1 - \frac{Q_{N,i}}{K_{N,i}}\right) = V_{m,N}\left(1 - \frac{N_{bio}}{\left(N_{prot} + N_{RNA}\right)K_{N,i}}\right) \tag{A.2}$$

Furthermore, setting the time derivative in Eq. (5) equal to 0:

$$y_N V_N N_{prot} - d N_{bio} = 0 \tag{A.3}$$

Combining (A.2) and (A.3) then gives:

$$V_{m,N} N_{prot} = \left(\frac{V_{m,N} N_{prot}}{\left(N_{prot} + N_{RNA}\right)K_{N,i}} + \frac{d}{y_N}\right) N_{bio} \tag{A.4}$$

and therefore:

$$N_{bio} = \frac{V_{m,N} N_{prot}}{\frac{V_{m,N} N_{prot}}{\left(N_{prot}+N_{RNA}\right)K_{N,i}} + \frac{d}{y_N}} = \frac{\left(\frac{V_{m,N} R_{N:P(RNA)} P_{in}}{b_0 + b_1 d}\right)}{\left(\frac{V_{m,N}}{(1+b_0+b_1 d)K_{N,i}} + \frac{d}{y_N}\right)} \tag{A.5}$$

To obtain an expression for C_{bio}, we set the time derivative in Eq. (9) equal to 0:

$$P_C - r_C - ex_C - co_{DON} - d C_{bio} = 0 \tag{A.6}$$

which gives with Eqs. (10) and (11):

$$C_{bio}\left(\frac{P_{m,C} N_{prot}}{K_{C,i}\left(N_{prot} + N_{RNA}\right)} + r_0 + r_1 d + d\right) = P_{m,C} N_{prot} - ex_C - co_{DON} \tag{A.7}$$

leading to:

$$C_{bio} = \frac{P_{m,C} N_{prot} - ex_C - co_{DON}}{\frac{P_{m,C} N_{prot}}{\left(N_{prot}+N_{RNA}\right)K_{C,i}} + r_0 + d(1+r_1)} = \frac{\left(P_{m,C} - \left(R_{C:N(DON)} + 2\right)(1-y_N)V_N\right)N_{prot}}{\frac{P_{m,C}}{(1+b_0+b_1 d)K_{C,i}} + r_0 + d(1+r_1)} \tag{A.8}$$

where we assumed that there is exudation of DON but not of DOP under P limitation, i.e., $ex_C = R_{C:N(DON)}(1\text{-}y_N)V_N N_{prot}$. Using Eqs. (A.5), (A.8), and $P_{bio} = P_{in}$, we calculate the C:N, C:P, and N:P ratios of the organisms, which are then fitted against the Elrifi and Turpin (1985) data.

To get an expression for N_{med}, we set the time derivative equal to 0 in Eq. (1):

$$N_{med} = N_{in} - \frac{V_N N_{prot}}{d} \approx N_{in} - V_{m,N}\left(1 - \frac{Q_{N,i}}{K_{N,i}}\right)\frac{R_{N:P(RNA)} P_{in}}{d(b_0 + b_1 d)} \tag{A.9}$$

A.2. N limitation

We assume that all N is in protein and RNA: $N_{prot} + N_{RNA} = N_{bio} = N_{in}$, giving with Eq. (12):

$$N_{prot} = \frac{N_{in}}{1 + \frac{N_{RNA}}{N_{prot}}} = \frac{N_{in}}{1 + b_0 + b_1 d} \tag{A.10}$$

P_{med} is very high (40–60 μM) under N limitation which means that Eq. (4) for the N uptake can be approximated as:

$$V_P \approx V_{m,P}\left(1 - \frac{Q_{P,i}}{K_{P,i}}\right) = V_{m,P}\left(1 - \frac{P_{bio}}{N_{in} K_{P,i}}\right) \tag{A.11}$$

Setting the time derivative in Eq. (6) equal to 0:

$$y_P V_P N_{prot} - d P_{bio} = 0 \tag{A.12}$$

Combining (A.11) and (A.12) gives:

$$V_{m,P} N_{prot} = \left(\frac{V_{m,P}}{(1 + b_0 + b_1 d)K_{P,i}} + \frac{d}{y_P}\right) P_{bio} \tag{A.13}$$

and therefore:

$$P_{bio} = \frac{V_{m,P}N_{prot}}{\frac{V_{m,P}}{(1+b_0+b_1 d)K_{P,i}} + \frac{d}{y_P}} = \frac{V_{m,P}N_{in}}{\frac{V_{m,P}}{K_{P,i}} + \frac{d(1+b_0+b_1 d)}{y_P}} \quad (A.14)$$

The expression for C_{bio} is the same as under P limitation (A.8), except that we now assume that there is exudation of DOP but not of DON, i.e., $ex_C = R_{C:P(DOP)}(1\text{-}y_P)V_P N_{prot}$:

$$C_{bio} = \frac{P_{m,C}N_{prot} - ex_C}{\frac{P_{m,C}N_{prot}}{K_{C,i}(N_{prot}+N_{RNA})} + r_0 + d(1+r_1)} = \frac{\left(P_{m,C} - R_{C:P(DOP)}(1-y_P)V_P\right)N_{prot}}{\frac{P_{m,C}}{K_{C,i}(1+b_0+b_1 d)} + r_0 + d(1+r_1)} \quad (A.15)$$

Using equations (A.8), (A.14), and $N_{bio} = N_{in}$, we calculate the C:N, C:P, and N:P ratios of the organisms, which are then fitted against the Elrifi and Turpin (1985) data.

To obtain an expression for P_{med}, we set the time derivative equal to 0 in Eq. (2):

$$P_{med} = P_{in} - \frac{V_P N_{prot}}{d} \approx P_{in} - \frac{V_{m,P}}{1 - \frac{Q_{P,i}}{K_{P,i}}} \frac{N_{in}}{(1 + b_0 + b_1 d)d} \quad (A.16)$$

Appendix B. Metropolis procedure

For parameter estimation in ocean plankton models, gradient methods have often been used (Gregg et al., 2009), such as the adjoint method (Fennel et al., 2001; Spitz et al., 2001; Faugeras et al., 2004) or the conjugate direction method (Fasham and Evans, 1995; Fasham et al., 1999; Hemmings et al., 2003). One disadvantage of gradient methods is that they tend to find the nearest optimum, which is not necessarily the global optimum. Therefore, if a global search method is computationally feasible for the optimization problem at hand, then a global search is preferable over a local search through a gradient method. Commonly used global optimization methods are random-walk Monte Carlo algorithms and genetic algorithms (Athias et al., 2000; Vallino, 2000).

We use a random-walk Monte Carlo method termed the "Metropolis algorithm" (Metropolis et al., 1953) that operates as follows:

1) A first guess is made for the parameter values using a priori knowledge about the system. From this first-guess parameter set, a new set of parameters is generated by random changes with a fixed standard deviation. Then, the model solution is calculated with this new parameter set.
2) For both the old and the new model solution, a sum-of-squared differences is calculated with respect to the experimental data. The exponent of the difference between these two sums-of-squares, scaled by the (assumed) uncertainty in the data, is the likelihood ratio of the two parameter sets. The new parameter set is adopted, if the likelihood ratio is larger than a random number between 0 and 1.
3) The algorithm wanders around the parameter space by repeating steps 1) and 2). Once the parameter distributions appear to have become stationary (usually after hundreds of thousands of iterations called the 'burn period'), a certain defined fraction of the parameter sets are stored. After a sufficient number of further iterations, means and standard deviations are calculated from these stored parameter sets.

New parameter sets are sometimes adopted when the likelihood ratio is below 1, which means that the new parameter set is somewhat worse than the old parameter set. During the burn period, this helps avoid getting stuck in local parameter optima. After the burn period, the algorithm focuses on the region around the global optimum. At this point, the goal is to obtain viable posterior distributions for the parameters. Therefore, we need to wander around in such a way that the amount of time spent in each location of parameter space is proportional to the likelihood of this set of parameters being correct. The way to do this is by flipping a coin that lands head with a probability equal to the likelihood ratio, which is the same as comparing the likelihood ratio with a random number from a uniform distribution between 0 and 1.

The Metropolis algorithm has previously been used to estimate parameters for biogeochemical models (Dowd, 2005; Lignell et al., 2013). In our view, one major advantage of the Metropolis algorithm is that it provides not only an estimate of the optimal parameter values, but also an estimate of the uncertainties in these parameter values. Another key advantage is that the procedure provides an effective safeguard against overfitting. If a model is not parsimonious with respect to the data it needs to describe, then the posterior parameter distributions become very broad and non-Gaussian.

Appendix C. Gross photosynthesis estimate

The high exudation rates of N and P are likely associated with a release also of C, as the C, N, and P are often part of the same molecule. Furthermore, the high DON release under P limitation requires the reduction of large amounts of NO_3^-. Can photosynthesis at the light intensity used in the Elrifi and Turpin (1985) experiments (100 µE/(m^2 s)) support such release?

To answer this question, we estimate the gross photosynthesis (P_C) at all dilution rates under N and P limitation by setting Eq. (9) equal to 0 (making the assumption that the culture is at steady state). Thus, we obtain:

$$P_C = r_C + ex_C + co_{DON} + dC_{bio} \quad (C.1)$$

This includes the impacts of respiration (r_C), exudation (ex_C), costs of NO_3^- reduction for DON production (co_{DON}), and dilution (dC_{bio}). In Fig. 5, the calculated gross photosynthesis is shown as a function of the dilution rate. It is lowest at low growth rates under N limitation (0.02 mM C/hr) and highest at high growth rates under P limitation (slightly over 0.2 mM C/hr). The Chl concentration at high growth rates under P limitation is about 0.4 mg Chl/l (Elrifi and Turpin, 1985), which means that the highest inferred gross photosynthesis rate was slightly over 0.2/0.4 = 0.5 mol C/(g Chl hr). Similar, and even higher, C fixation rates have been observed in cultures under 100 µE/(m^2 s) (e.g., Platt et al., 1980; Harding et al., 1982; Felcmanová et al., 2017). Note that the gross photosynthesis is actually higher than these measured C fixation rates, which do not include respiration. These rates are also reasonable from a biochemical perspective. Most reported values for the turnover number of Rubisco (k_{cat}) are in the range of 1–4 mol C/(mol binding sites s) for both algae and (C3) land plants (Seemann and Sharkey, 1986; Uemura et al., 1997; Zhu et al., 1998; Sage, 2002; Parry et al., 2007; Kubien et al., 2008; Pérez et al., 2011; Galmés et al., 2014; Hermida-Carrera et al., 2016; Orr et al., 2016; Young et al., 2016; Atkinson et al., 2017). To convert these k_{cat} values into maximum C-fixation rates, we multiply them by 0.06 mmol binding sites/(g Chl), the amount of binding sites per amount of Chl in *Selenastrum minutum*, as measured by Elrifi et al. (1988). This gives 0.06–0.24 mmol C/(g Chl s) or (0.06–0.24)*10^{-3} × 3600=0.2–0.9 mol C/(g Chl hr), right around the predicted value of 0.5 mol C/(g Chl hr). Hence, two different lines of empirical evidence suggest that our estimated rates of DOM production are not implausible.

Elrifi and Turpin (1986) also reported a photosynthesis rate of 0.151 mol C/(g Chl hr), measured at a growth rate of 0.3 per day under N limitation and 100 µE/(m^2 s) light. Our model predicts a photosynthesis rate of just over 0.025 mM C/hr at a growth rate of 0.3 per day under N limitation (see Fig. 5a). This corresponds to 0.025/(0.1 × 12.5) = 0.02 mol C/(mol C hr), given that the C:N ratio is about 12.5 (Fig. 3e) and the N concentration is 0.1 mM. With

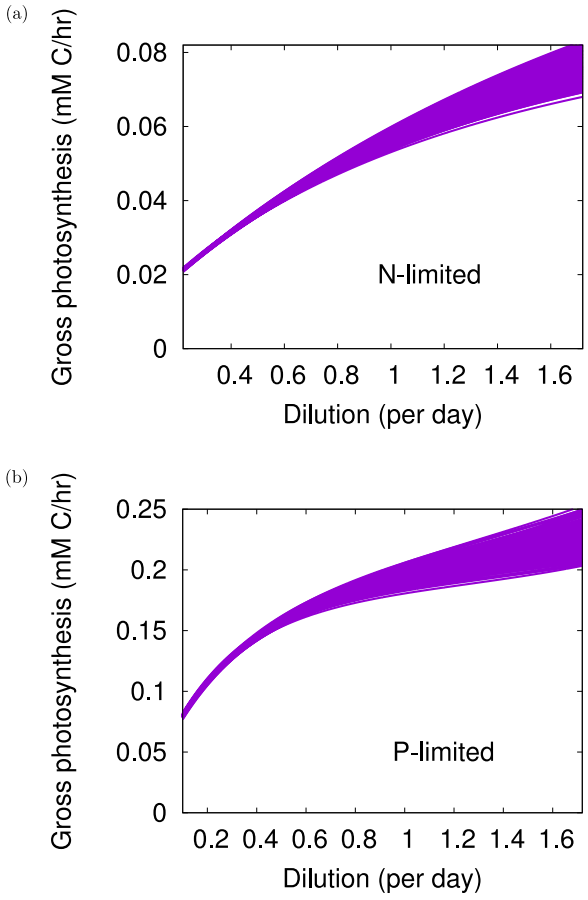

Fig. 5. Calculated gross photosynthesis rate (mM C/hr) under N limitation (a) and under P limitation (b).

~8 mol C/(g Chl) at this growth rate under N limitation (Fig. 4 in Elrifi and Turpin, 1985), this corresponds to ~8 × 0.02 = ~0.16 mol C/(g Chl hr), similar to the reported 0.151 mol C/(g Chl hr).

The parameter estimate indicates relatively low values for the C:N ratio of the DON exuded under P limitation and the C:P ratio of the DOP exuded under N limitation (3.1 ± 0.4 and 6.6 ± 0.9, respectively) that may be due to the extreme N:P ratios of the input. However, we note that the C:N and C:P ratios of the exuded material are relatively weakly constrained, since the mass budget for C is not as strongly constrained as the mass budgets for N and P. Therefore, we have performed sensitivity calculations. If we increase the C:N and C:P ratios of the exuded material up to the Redfield ratio (in accordance with Saad et al., 2016), the gross photosynthesis is still no higher than 1 mol C/(g Chl hr) at the highest growth rates. This is well within the C fixation range previously measured at 100 µE/(m^2 s) (Harding et al., 1982).

References

Admiraal, W., Peletier, H., Laane, R.W.P.M., 1986. Nitrogen metabolism of marine planktonic diatoms; excretion, assimilation and cellular pools of free amino acids in seven species with different cell size. J. Exp. Mar. Biol. Ecol. 98, 241–263.

Athias, V., Mazzega, P., Jeandel, C., 2000. Selecting a global optimization method to estimate the oceanic particle cycling rate constants. J. Mar. Res. 58, 675–707.

Atkinson, N., Leitão, N., Orr, D.J., Meyer, M.T., Carmo-Silva, E., Griffiths, H., Smith, A.M., McCormick, A.J., 2017. Rubisco small subunits from the unicellular green alga *Chlamydomonas* complement Rubisco-deficient mutants of *Arabidopsis*. New Phytol. 214, 655–667.

Anderson, T.R., Pondaven, P., 2003. Non-Redfield carbon and nitrogen cycling in the Sargasso sea: pelagic imbalances and export flux. Deep-Sea Res. I 50, 573–591.

Barica, J., 1990. Seasonal variability of N:P ratios in eutrophic lakes. Hydrobiologia 191, 97–103.

Basan, M., Hui, S., Okano, H., Zhang, Z., Shen, Y., Williamson, J.R., Hwa, T., 2015. Overflow metabolism in *Escherichia coli* results from efficient protein allocation. Nature 528, 99–104.

Benitez-Nelson, C.R., Buesseler, K.O., 1999. Variability of inorganic and organic phosphorus turnover rates in the coastal ocean. Nature 398, 502–505.

Benitez-Nelson, C.R., 2000. The biogeochemical cycling of phosphorus in marine systems. Earth-Sci. Rev. 51, 109–135.

Berman-Frank, I., Dubinsky, Z., 1999. Balanced growth in aquatic plants: myth or reality? Bioscience 49, 29–37.

Bergman, B., 1984. Photorespiratory ammonium release by the cyanobacterium *Anabaena cylindrica* in the presence of methionine sulfoximine. Arch. Microbiol. 137, 21–25.

Biddanda, B., Benner, R., 1997. Carbon, nitrogen, and carbohydrate fluxes during the production of particulate and dissolved organic matter by marine phytoplankton. Limnol. Oceanogr. 42, 506–518.

Biller, S.J., Schubotz, F., Roggensack, S.E., Thompson, A.W., Summons, R.E., Chisholm, S.W., 2014. Bacterial vesicles in marine ecosystems. Science 343, 183–186.

Björkman, K.M., Duhamel, S., Karl, D.M., 2012. Microbial group specific uptake kinetics of inorganic phosphate and adenosine-5'-triphosphate (ATP) in the North Pacific subtropical gyre. Front. Microbiol. 3, 189.

Björkman, K.M., Karl, D.M., 2003. Bioavailability of dissolved organic phosphorus in the euphotic zone at station ALOHA, North Pacific subtropical gyre. Limnol. Oceanogr. 48, 1049–1057.

Björkman, K.M., Thomson-Bulldis, A.L., Karl, D.M., 2000. Phosphorus dynamics in the North Pacific subtropical gyre. Aquat. Microb. Ecol. 22, 185–198.

Bougaran, G., Bernard, O., Sciandra, A., 2010. Modeling continuous cultures of microalgae colimited by nitrogen and phosphorus. J. Theor. Biol. 265, 443–454.

Boulion, V.V., 2012. Assimilation and turnover time of phosphorus by size fractions of microplankton in lakes of different types. Inland Water Biol 5, 11–16.

Boyer, K.E., Fong, P., Armitage, A.R., Cohen, R.A., 2004. Elevated nutrient content of tropical macroalgae increases rates of herbivory in coral, seagrass, and mangrove habitats. Coral Reefs 23, 530–538.

Bronk, D.A., 1999. Rates of NH_4^+ uptake, intracellular transformation and dissolved organic nitrogen release in two clones of marine *Synechococcus* spp. J. Plankton Res. 21, 1337–1353.

Caperon, J., Meyer, J., 1972. Nitrogen-limited growth of marine phytoplankton – Changes in population characteristics with steady-state growth rate. Deep-Sea Res 19, 601–618.

Clark, D.R., 1998. Carbon-nitrogen stress and the growth of marine phytoplankton Ph.D. thesis. University of Wales, UK.

Cook, J.R., 1963. Adaptations in growth and division in *Euglena* effected by energy supply. J. Protozool. 10, 436–444.

Del Giorgio, P.A., Cole, J.J., 1998. Bacterial growth efficiency in natural aquatic systems. Annu. Rev. of Ecol. Evol. S. 29, 503–541.

Diaz, J.M., Björkman, K.M., Haley, S.T., Ingall, E.D., Karl, D.M., Longo, A.F., Dyhrman, S.T., 2016. Polyphosphate dynamics at station ALOHA, North Pacific subtropical gyre. Limnol. Oceanogr. 61, 227–239.

Donald, K.M., Joint, I., Rees, A.P., Woodward, E.M.S., Savidge, G., 2001. Uptake of carbon, nitrogen and phosphorus by phytoplankton along the 20°W meridian in the NE Atlantic between 57.5°N and 37°N. Deep-Sea Res. II 48, 873–897.

Dowd, M., 2005. A sequential Monte Carlo approach for marine ecological prediction. Environmetrics 17, 435–455.

Droop, M.R., 1968. Vitamin B_{12} and marine ecology. IV. The kinetics of uptake, growth and inhibition in *Monochrysis lutheri*.. J. Mar. Biol. Assoc. UK 48, 689–733.

Dyhrman, S.T., 2016. Nutrients and their acquisition: phosphorus physiology in microalgae. In: Borowitzka, M.A., Beardall, M.A., Raven, J.A. (Eds.), The Physiology of Microalgae. Springer International, Switzerland, pp. 155–183.

Elrifi, I.R., Holmes, J.J., Weger, H.G., Mayo, W.P., Turpin, D.H., 1988. RuBP limitation of photosynthetic carbon fixation during NH_3 assimilation. Plant Physiol 87, 395–401.

Elrifi, I.R., Turpin, D.H., 1985. Steady-state luxury consumption and the concept of optimum nutient ratios: a study with phosphate and nitrate limited *Selenastrum minutum* (Chlorophyta). J. Phycol. 21, 592–602.

Elrifi, I.R., Turpin, D.H., 1986. Nitrate and ammonium induced photosynthetic suppression in N-limited *Selenastrum minutum* (Chlorophyta). Plant Physiol 81, 273–279.

Elser, J.J., Dobberfuhl, D.R., MacKay, N.A., Schampel, J.H., 1996. Organism size, life history, and N:P stoichiometry Bioscience 46, 674–684.

Eysseltova, J., Dirkse, T.P., 1988. Solubility Data series, Vol. 31: Alkali Metal Orthophosphates. International Union of Pure and Applied Chemistry, Zürich, Switzerland.

Fasham, M.J.R., Boyd, P.W., Savadge, G., 1999. Modeling the relative contributions of autotrophs and heterotrophs to carbon flow at a Lagrangian JGOFS station in the Northeast Atlantic: the importance of DOC. Limnol. Oceanogr. 44, 80–94.

Fasham, M.J.R., Ducklow, H.W., McKelvie, S.M., 1990. A nitrogen-based model of plankton dynamics in the oceanic mixed layer. J. Mar. Res. 48, 591–639.

Fasham, M.J.R., Evans, G.T., 1995. The use of optimization techniques to model marine ecosystem dynamics at the JGOFS station at 47°N 20°W. Philos. Trans. Royal Soc. B 348, 203–209.

Faugeras, B., Bernard, O., Sciandra, A., Lévy, M., 2004. A mechanistic modelling and data assimilation approach to estimate the carbon/chlorophyll and carbon/nitrogen ratios in a coupled hydrodynamical-biological model. Nonlinear Process. Geophys. 11, 515–533.

Felcmanová, K., Lukes, M., Kotabová, E., Lawrenz, E., Halsey, K.H., Prásil, O., 2017. Carbon use efficiencies and allocation strategies in *Prochlorococcus marinus* strain PCC 9511 during nitrogen-limited growth. Photosynth. Res. 134, 71–82.

Fennel, K., Losch, M., Schroter, J., Wenzel, M., 2001. Testing a marine ecosystem model: sensitivity analysis and parameter optimization. J. Mar. Sys. 28, 45–63.

Flynn, K.J., 2008. The importance of the form of the quota curve and control of non-limiting nutrient transport in phytoplankton models. J. Plankton Res. 30, 423–438.

Flynn, K.J., Clark, D.R., Xu, Y., 2008. Modeling the release of dissolved organic matter by phytoplankton. J. Phycol. 44, 1171–1187.

Flynn, K.J., Raven, J.A., Rees, T.A.V., Finkel, Z., Quigg, A., Beardall, J., 2010. Is the growth rate hypothesis applicable to microalgae? J. Phycol. 46, 1–12.

Galmés, J., Kapralov, M.V., Andraloic, P.J., Conesa, M.À., Keys, A.J., Parry, M.A.J., Flexas, J., 2014. Expanding knowledge of the Rubisco kinetics variability in plant species: environmental and evolutionary trends. Plant, Cell Environ 37, 1989–2001.

Gauthier, D.A., Turpin, D.H., 1997. Interactions between inorganic phosphate (Pi) assimilation, photosynthesis and respiration in the Pi-limited green alga *Selenastrum minutum*. Plant, Cell Environ. 20, 12–24.

Geider, R.J., MacIntyre, H.J., Kana, T.M., 1998. A dynamic regulatory model of phytoplanktonic acclimation to light, nutrients and temperature. Limnol. Oceanogr. 43, 679–694.

Geider, R.J., Osborne, B.A., 1989. Respiration and microalgal growth: a review of the quantitative relationship between dark respiration and growth. New Phytol 112, 327–341.

Ghyoot, C., Flynn, K.J., Mitra, A., Lancelot, C., Gypens, N., 2017. Modeling plankton mixotrophy: a mechanistic model consistent with the shuter-type biochemical approach. Front. Ecol. Evol. 5, 78.

Grant, S.R., Bienfang, P.K., Laws, E.A., 2013. Steady-state bioassay approach applied to phosphorus-limited continuous culture: a growth study of the marine chlorophyte *Dunaliella salina*. Limnol. Oceanogr. 58, 314–324.

Gregg, W.W., Friedrichs, M.A.M., Robinson, A.R., Rose, K.A., Schlitzer, R., Thompson, K.R., Doney, S.C., 2009. Skill assessment in ocean biological data assimilation. J. Mar. Sys. 76, 16–33.

Grossowicz, M., Roth-Rosenberg, D., Aharonovich, D., Silverman, J., Follows, M.J., Sher, D., 2017a. *Prochlorococcus* in the lab and in silico: the importance of representing exudation. Limnol. Oceanogr. 62, 818–835.

Grossowicz, M., Marques, G.M., Van Voorn, G.A.K., 2017b. A dynamic energy budget (DEB) model to describe population dynamics of the marine cyanobacterium *Prochlorococcus marinus*. Ecol. Model. 359, 320–332.

Halmann, M., Stiller, M., 1974. Turnover and uptake of dissolved phosphate in freshwater. A study in Lake Kinneret. Limnol. Oceanogr. 19, 774–783.

Hammer, K.D., Brockmann, U.H., 1983. Rhythmic release of dissolved free amino acids from partly synchronized *Thalassiosira rotula* under nearly natural conditions. Mar. Biol. 74, 305–312.

Harding, L.W., Prézelin, B.B., Sweeney, B.M., Cox, J.L., 1982. Diel oscillations of the photosynthesis-irradiance (*P-I*) relationship in natural assemblages of phytoplankton. Mar. Biol. 67, 167–178.

Healey, F.P., 1985. Interacting effects of light and nutrient limitation on the growth of *Synechococcus linearis* (Cyanophyceae). J. Phycol. 21, 134–146.

Hemmings, J.C.P., Srokosz, M.A., Challenor, Fasham, M.J.R., 2003. Assimilating satellite ocean-colour observations into oceanic ecosystem models. Philos. Trans. Royal Soc. A 361, 33–39.

Hermida-Carrera, C., Kapralov, M.V., Galmés, J., 2016. Rubisco catalytic properties and temperature response in crops. Plant Physiol 171, 2549–2561.

Hessen, D.O., Elser, J.J., Sterner, R.W., Urabe, J., 2013. Ecological stoichiometry: an elementary approach using basic principles. Limnol. Oceanogr. 58, 2219–2236.

Jansson, M., 1993. Uptake, exchange, and excretion of orthophosphate in phosphate-starved *Scenedesmus quadricauda* and *Pseudomonas* K7. Limnol. Oceanogr. 38, 1162–1178.

Karl, D.M., 2014. Microbially mediated transformations of phosphorus in the sea: new views of an old cycle. Ann. Rev. Mar. Sci. 6, 279–337.

Karl, D.M., Björkman, K.M., 2015. Dynamics of dissolved organic phosphorus. In: Hansell, D.A., Carlson, C.A. (Eds.), Biogeochemistry of Marine Dissolved Organic Matter, 2nd ed. Elsevier Inc, The Netherlands, pp. 233–334.

Klausmeier, C.A., Litchman, E., Daufresne, T., Levin, S.A., 2004. Optimal nitrogen–to-phosphorus stoichiometry of phytoplankton. Nature 429, 171–174.

Koistinen, J., Sjöblom, M., Spilling, K., 2020. Determining inorganic and organic phosphorus. Methods in Molecular Biology, 1980. Humana Press, pp. 87–94.

Kooijman, S.A.L.M., 2010. Dynamic Energy Budget Theory For Metabolic Organisation, 3rd ed. Cambridge University Press, Cambridge, UK.

Körtzinger, A., Koeve, W., Kähler, P., Mintrop, L., 2001. C:N ratios in the mixed layer during the productive season in the Northeast Atlantic ocean. Deep-Sea Res. I 48, 661–688.

Kubien, D.S., Whitney, S.M., Moore, P.V., Jesson, L.K., 2008. The biochemistry of Rubisco in *Flaveria*. J. Exp. Bot. 59, 1767–1777.

Laws, E.A., Bidigare, R.R., Karl, D.M., 2016. Enigmatic relationship between chlorophyll-a concentrations and photosynthetic rates at Station ALOHA. Heliyon 2, e00156.

Laws, E.A., Pei, S., Bienfang, P.K., 2013. Phosphate-limited growth of the marine diatom *Thalassiosira weissflogii*: evidence of non-Monod growth kinetics. J. Phycol. 49, 241–247.

Legovic, T., Cruzado, A., 1997. A model of phytoplankton growth on multiple nutrients based on the Michaelis-Menten-Monod uptake, Droop's growth and Liebig's law. Ecol. Model. 99, 19–31.

Lignell, R., Haario, H., Laine, M., Thingstad, T.F., 2013. Getting the "right" parameter values for models of the pelagic microbial food web. Limnol. Oceanogr. 58, 301–313.

Lin, S., Litaker, R.W., Sunda, W.G., 2016. Phosphorus physiological ecology and molecular mechanisms in marine phytoplankton. J. Phycol. 52, 10–36.

Litchman, E., Nguyen, B.L.V., 2008. Alkaline phosphatase activity as a function of internal phosphorus concentration in freshwater phytoplankton. J. Phycol. 52, 1379–1383.

Livanou, E., Lagaria, A., Psarra, S., Lika, K., 2019. A DEB-based approach to dissolved organic matter release by phytoplankton. J. Sea Res. 143, 140–151.

Li, H.M., Zhang, Y.Y., Han, X.R., Shi, X.Y., Rivkin, R.B., Legendre, L., 2016. Growth responses of *Ulva prolifera* to inorganic and organic nutrients: implications for macroalgal blooms in the Southern Yellow Sea, China. Sci. Rep. 6 (26), 498.

Lønborg, C., Martinez-Garcia, S., Teira, E., Alvarez-Salgado, X.A., 2011. Bacterial carbon demand and growth efficiency in a coastal upwelling system. Aquat. Microb. Ecol. 63, 183–191.

Lorena, A., Marques, G.M., Kooijman, S.A.L.M., Sousa, T., 2010. Stylized facts in microalgal growth: interpretation in a dynamic energy budget context. Philos. Trans. Roy. Soc. B 365, 3509–3521.

Majewski, R.A., Domach, M.M., 1990. Simple constrained-optimization view of acetate overflow in *E. coli*. Biotechnol. Bioeng. 35, 732–738.

Martin, P., Dyhrman, S.T., Lomas, M.W., Poulton, N.J., Van Mooy, B.A.S., 2014. Accumulation and enhanced cycling of polyphosphate by Sargasso Sea plankton in response to low phosphorus. Proc. Natl. Acad. Sci. USA 111, 8089–8094.

Martiny, A.C., Vrugt, J.A., Primeau, F.W., Lomas, M.W., 2013. Regional variation in the particulate organic carbon to nitrogen ratio in the surface ocean. Glob. Biogeochem. Cyc. 27, 723–731.

Metropolis, N., Rosenbluth, A.W., Rosenbluth, M.N., Teller, A.H., Teller, E., 1953. Equations of state calculations by fast computing machines. J. Chem. Phys. 21, 1087–1092.

Meza, B., De-Bashan, L.E., Hernandez, J.P., Bashan, Y., 2015. Accumulation of intracellular polyphosphate in *Chlorella vulgaris* cells is related to indole-3-acetic acid produced by *Azospirillum brasilense*. Res. Microbiol. 5, 399–407.

Molenaar, D., Van Berlo, R., De Ridder, D., Teusink, B., 2009. Shifts in growth strategies reflect tradeoffs in cellular economics. Mol. Syst. Biol. 5, 323.

Moody, E.K., Rugenski, A.T., Sabo, J.L., Turner, B.L., Elser, J.J., 2017. Does the growth rate hypothesis apply across temperatures? Variation in the growth rate and body phosphorus of neotropical benthic grazers. Front. Environ. Sci. 5, 14.

Moreno, A.R., Martiny, A.C., 2018. Ecological stoichiometry of ocean plankton. Ann. Rev. Mar. Sc. 10, 43–69.

Myklestad, S.M., Holm-Hansen, O., Varum, K.M., Volcani, B.E., 1989. Rate of release of extracellular amino acids and carbohydrates from the marine diatom *Chaetoceros affinis*. J. Plankton Res. 11, 763–773.

Nagao, F., Miyazaki, T., 2002. Release of dissolved organic nitrogen from *Scenedesmus quadricauda* (Chlorophyta) and *Microcystis novacekii* (Cyanobacteria). Aquat. Microb. Ecol. 27, 275–284.

Nausch, M., Nausch, G., 2006. Bioavailability of dissolved organic phosphorus in the Baltic Sea. Mar. Ecol.: Prog. Ser. 321, 9–17.

Nowlin, W.H., Davies, J.M., Mazumder, A., 2007. Planktonic phosphorus pool sizes and cycling efficiency in coastal and interior British Columbia lakes. Freshwater Biol 52, 860–877.

Omta, A.W., Talmy, D., Sher, D., Finkel, Z.V., Irwin, A.D., Follows, M.J., 2017. Extracting phytoplankton physiological traits from batch and chemostat culture data. Limnol. Oceanogr.: Methods 15, 453–466.

Orchard, E.D., Benitez-Nelson, C.R., Pellechia, P.J., Lomas, M.W., Dyhrman, S.T., 2010. Polyphosphate in *Trichodesmium* from the low-phosphorus Sargasso Sea. Limnol. Oceanogr. 55, 2161–2169.

Orr, D.J., Alcântara, A., Kapralov, M.V., Andralojc, P.J., Carmo-Silva, E., Parry, M.A.J., 2016. Surveying Rubisco diversity and temperature response to improve crop photosynthetic efficiency. Plant Physiol. 172, 707–717.

Orth, J.D., Thiele, I., Palsson, B.O., 2010. What is flux balance analysis? Nat. Biotechnol. 28, 245–248.

Pacheco, A.R., Moel, M., Segrè, D., 2019. Costless metabolic secretions as drivers of interspecies interactions in microbial ecosystems. Nat. Commun. 10, 103.

Pahlow, M., 2005. Linking chlorophyll-nutrient dynamics to the Redfield N:C ratio with a model of optimal phytoplankton growth. Mar. Ecol.: Prog. Ser. 287, 33–43.

Pahlow, M., Vézina, A.F., Casault, B., Maass, H., Malloch, L., Wright, D.G., Lu, Y., 2008. Adaptive model of plankton dynamics for the North Atlantic. Prog. Oceanogr. 76, 151–191.

Pahlow, M., Oschlies, A., 2009. Chain model of phytoplankton P, N, and light colimitation. Mar. Ecol.: Prog. Ser. 376, 69–83.

Palenik, B., Morel, F.M.M., 1991. Amine oxidases of marine phytoplankton. Appl. Environ. Microbiol. 57, 2440–2443.

Pantoja, S., Lee, C., 1994. Cell-surface oxidation of amino acids in sea water. Limnol. Oceanogr. 39, 1718–1726.

Parry, M.A.J., Madgwick, P.J., Carvallo, J.F.C., Andralojc, P.J., 2007. Prospects for increasing photosynthesis by overcoming the limitations of Rubisco. J. Agric. Sci. 145, 31–43.

Paytan, A., McLaughlin, K., 2007. The oceanic phosphorus cycle. Chem. Rev. 107, 563–576.

Pérez, P., Alonso, A., Zita, G., Morcuende, R., Martínez-Carrasco, R., 2011. Down-regulation of Rubisco activity under combined increases of CO_2 and temperature minimized by changes in Rubisco k_{cat} in wheat. Plant Growth Regul 65, 439–447.

Peters, R.H., MacIntyre, S., 1976. Orthophosphate turnover in East African lakes. Oecologia 25, 313–319.
Plath, K., Boersma, M., 2001. Mineral limitation of zooplankton: stoichiometric constraints and optimal foraging. Ecology 82, 1260–1269.
Platt, T., Gallegos, C.L., Harrison, W.G., 1980. Photoinhibition of photosynthesis in natural assemblages of marine phytoplankton. J. Mar. Res. 38, 687–701.
Powell, N., Shilton, A., Pratt, S., Chisti, Y., 2011. Phosphate release from waste stabilisation pond sludge: significance and fate of polyphosphate. Water Sci. Technol. 63, 1689–1694.
Ranhofer, M.L., Lawrenz, E., Pinckney, J.L., Benitez-Nelson, C.R., Richardson, T.L., 2009. Cell-specific alkaline phosphatase expression by phytoplankton from Winyah Bay, South Carolina, USA. Estuaries Coasts 32, 943–957.
Raven, J.A., 1984. MBL Lectures in Biology, Volume 4: Energetics and Transport in Aquatic Plants. Alan R. Liss, Inc., New York.
Redfield, A.C., 1934. On the proportions of organic derivatives in sea water and their relation to the composition of plankton. In: Daniel, R.J. (Ed.), James Johnstone Memorial Volume. Liverpool University Press, Liverpool, UK, pp. 176–192.
Rhee, G.Y., 1973. A continuous culture study of phosphate uptake, growth rate and polyphosphate in *Scenedesmus* sp. J. Phycol. 9, 495–506.
Rhee, G.Y., 1974. Phosphate uptake under nitrogen limitation by *Scenedesmus* sp. and its ecological implications. J. Phycol. 10, 470–475.
Rhee, G.Y., 1978. Effects of N:P limitation on algal growth, cell composition, and nitrate uptake. Limnol. Oceanogr. 23, 10–24.
Rich, P.R., 2003. The molecular machinery of Keilin's respiratory chain. Biochem. Soc. Trans. 31, 1095–1105.
Rieger, M., Kappeli, O., Flechter, A., 1983. The role of limited respiration in the incomplete oxidation of glucose by *Saccharomyces cerevisae*. J. Gen. Microbiol. 52, 653–661.
Rigler, F.H., 1964. The phosphorus fractions and the turnover time of inorganic phosphorus in different types of lakes. Limnol. Oceanogr. 9, 511–518.
Ruttenberg, K.C., Dyhrman, S.T., 2012. Dissolved organic phosphorus production during simulated phytoplankton blooms in a coastal upwelling system. Front Microbiol 3, 274.
Saad, E.M., Longo, A.F., Chambers, L.R., Huang, R., Benitez-Nelson, C., Dyhrman, S.T., Diaz, J.M., Tang, Y., Ingall, E.D., 2016. Understanding marine dissolved organic matter production: compositional insights from axenic cultures of *Thalassiosira pseudonana*. Limnol. Oceanogr. 61, 2222–2233.
Sage, R.F., 2002. Variation in the k_{cat} of Rubisco in C3 and C4 plants and some implications for photosynthetic performance at high and low temperature. J. Exp. Bot. 53, 609–620.
Scott, M., Gunderson, C.W., Matescu, E.M., Zhang, Z., Hwa, T., 2010. Interdependence of cell growth and gene expression: origins and consequences. Science 330, 1099–1102.
Seemann, J.R., Sharkey, T.D., 1986. Salinity and nitrogen effects on photosynthesis, ribulose-1,5-bisphosphate carboxylase and metabolite pool sizes in *Phaseolus vulgaris* l. Plant Physiol 82, 555–560.
Shuter, B., 1979. A model of physiological adaptation in unicellular algae. J. Theor. Biol. 78, 519–552.
Singh, A., Baer, S.E., Riebesell, U., Martiny, A.C., Lomas, M.W., 2015. C:N:P stoichiometry at the Bermuda Atlantic time-series study station in the North Atlantic Ocean. Biogeosciences 12, 6389–6403.
Sipler, R.E., Bronk, D.A., 2015. Dynamics of dissolved organic nitrogen. In: Hansell, D.A., Carlson, C.A. (Eds.), Biogeochemistry of Marine Dissolved Organic Matter. Elsevier Inc, The Netherlands, pp. 127–232.
Smith, S.L., Yamanaka, Y., 2007. Optimization model of multi-nutrient uptake kinetics. Limnol. Oceanogr. 51, 874–883.
Sohm, J.A., Capone, D.G., 2010. Zonal differences in phosphorus pools, turnover and deficiency across the tropical North Atlantic Ocean. Glob. Biogeochem. Cycles 24, GB2008.
Sonnleitner, B., Kappeli, O., 1986. Growth of *Saccharomyces cerevisae* is controlled by its limited respiratory capacity: formulation and verification of a hypothesis. Biotechnol. Bioeng. 28, 927–937.
Spitz, Y.H., Moisan, J.R., Abott, M.R., 2001. Configuring an ecosystem model using data from the Bermuda Atlantic time series (BATS). Deep-Sea Res. II 48, 1733–1768.
Sterner, R.W., Elser, J.J., 2002. Ecological Stoichiometry. Princeton University Press, Princeton.
Szenk, M., Dill, K.A., De Graff, A.M.R., 2017. Why do fast-growing bacteria enter overflow metabolism? Testing the membrane real estate hypothesis. Cell Syst 2, 95–104.
Taylor, W.D., Lean, D.R.S., 1981. Radiotracer experiments on phosphorus uptake and release by limnetic microzooplankton. Can. J. Fish. Aquat. Sci. 38, 1316–1321.
Terry, K.L., Hirata, J., Laws, E.A., 1985. Light-, nitrogen, and phosphorus-limited growth of *Phaeodactylum tricornutum* Bohlin strain TFX-1: chemical composition, carbon partitioning, and the diel periodicity of physiological processes. J. Exp. Mar. Biol. Ecol. 86, 85–100.
Uemura, K., Anwaruzzaman, Miyachi, S., Yokota, A., 1997. Ribulose-1,5-Bisphosphate carboxylase/oxygenase from thermophilic red algae with a strong specificity for CO_2 fixation. Biochem. Biophys. Res. Commun. 233, 568–571.
Vallino, J.J., 2000. Improving marine ecosystem models: use of data assimilation and mesocosm experiments. J. Mar. Res. 58, 117–164.
Van Mooy, B.A.S., et al., 2015. Major role of planktonic phosphate reduction in the marine phosphorus cycle. Science 348, 783–785.
Varma, A., Palsson, B.O., 1994. Metabolic flux balancing: basic concepts, scientific and practical use. Bio/Technol 12, 994–998.
Vrede, T., Dobberfuhl, D.R., Kooijman, S.A.L.M., Elser, J.J., 2004. Fundamental connections among organism C:N:P stoichiometry, macromolecular composition, and growth. Ecol 85, 1217–1229.
Weger, H.G., Birch, D.G., Elrifi, I.R., Turpin, D.H., 1988. Ammonium assimilation requires mitochondrial respiration in the light: a study with the green alga *Selenastrum minutum*. Plant Physiol. 86, 688–692.
Werner, T.P., Amrhein, N., Freimoser, F.M., 2007. Inorganic polyphosphate occurs in the cell wall of *Chlamydomonas reinhardtii* and accumulates during cytokinesis. BMC Plant. Biol. 7, 51.
Young, J.N., Heureux, A.M.C., Sherwood, R.E., Rickaby, R.E.M., Morel, F.M.M., Whitney, S.M., 2016. Large variation in the Rubisco kinetics of diatoms reveals diversity among their carbon-concentrating mechanisms. J. Exp. Bot. 67, 313–319.
Zhu, G., Jensen, R.G., Bohnert, H.J., Wildner, G.F., Schlitter, J., 1998. Dependence of catalysis and CO_2/O_2 specificity of Rubisco on the carboxy-terminus of the large subunit at different temperatures. Photosynth. Res. 57, 71–79.